

Electrical Potential Distribution in Polymethyl Methacrylate-Graphene Oxide Nanocomposites

Z. Nawawi¹, R. F. Kurnia², N. F. A. Isa³, Z. Buntat⁴, D. R. Yuniarti⁵, M. I. Jambak⁶,
M. A. B. Sidik^{*7}

^{1,5,6,7}Department of Electrical Engineering, Faculty of Engineering, Universitas Sriwijaya,
Ogan Ilir, South Sumatra, Indonesia

^{2,3,4}Institute of High Voltage and High Current (IVAT), Faculty of Electrical Engineering,
Universiti Teknologi Malaysia, 81310 UTM Johor Bahru, Malaysia

*Corresponding author, email: abubakar@unsri.ac.id

Abstract

Research work of polymer nanocomposites in high voltage insulator becomes interest nowadays. Polymer based and nanofillers are the core components in polymer nanocomposites. By adding such a big amount of nanofiller it would enhance the electrical and mechanical properties of polymers. However as for today, a little percentage of nanofiller concentration could dramatically enhanced the properties of the polymeric material. Recent research of graphene oxide (GO) nanofiller has brought to this project interest. This paper presents several methods that have been published to development PMMA (poly methyl methacrylate)/GO nanocomposites and a simulation of PMMA/GO in order to investigate the potential distribution.

Keywords: nanocomposites, graphene oxide, PMMA

Copyright © 2016 Institute of Advanced Engineering and Science. All rights reserved.

1. Introduction

The interest of polymer nanocomposites in academic and industry research have emerged and lead to wide discoveries of various fields such as biomedical, chemical, electrical and electronics. Polymer composite is the science of mixing the polymers such as polystyrene, polyethylene, polypropylene with other chemicals (nanofillers) in order to produce a polymer composite. Nanofillers are used to reinforce the base polymer, which can increase the physical properties or play the role of certain processing characteristics. The reinforcing type nanofiller can improve tensile strength, modulus, tear strength and corrosion resistance of a compound.

Graphene oxide nanofiller is formed from the oxidation of graphite. Graphite is a three-dimensional carbon based material made up of millions of layers of graphene. Thus, graphene oxide is potential advanced nanofiller, which can dramatically improve the dielectric properties of polymer-based composite. The outstanding electrical and physical properties of graphene derivatives have made an enormous impact among researchers during past few years. Integration of individual graphene oxide and polymer nanocomposite thus will take advantage as one of the well-matched integration as to improve insulating performance of the insulator.

In high voltage insulation system, Partial Discharge (PD) will cause a gradual erosion and reduction on an insulator thickness, which is leading to breakdown of the insulator. To overcome this problem, the dielectric materials need to be improved so that they life span service could be longer. Recent research activities reveal that by adding a little percentage of nanofiller concentration the properties of polymeric material could be improved drastically. This paper are to review and simulate the performance of PMM-GO nanocomposite in high voltage system.

2. Past Research on Graphene Oxide

Graphene is a potential industrial application since it has extraordinary electronic transport properties. The investigation on mechanical properties of the exfoliation of graphite with polymer composite compared to single wall carbon nanotube (SWNT) polystyrene composite that was made by latex technology has shown the same results. However, graphene

sheet have higher surface-to-volume ratios than SWNT'S composite, make it the most potentially favorable study material in polymer matrix properties alteration [1].

The Lef-Klinowski model is the most likely presenting the GO structure. The model is described as in Figure 1 where it is built of pristine aromatic "islands" separated by epoxide and hydroxyl groups and double bonds. It is also stated that GO is electrically insulating hence process of reducing it is required to restore electrical conductivity [2].

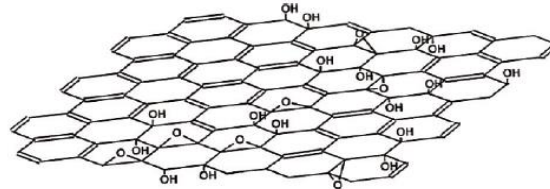


Figure 1. Structure of GO Described by Lef Klinowski Model [2].

The characteristics of graphene oxide paper was determined by tensile test and bending test. Very high values of tensile modulus and fracture strength were obtained from the tensile test measurements. Graphene oxide paper is stronger than traditional carbon and a clay-based paper since it is able to endure tribulation with low cracking. As a result, it could be served as a carrier substance in order to produce hybrid material comprising ceramics, metals and of course polymers [3].

Xingyi Huang et al [4] investigated the graphene oxide as an insulating material. The experiment was conducted using such measurements that are FTIR, TGA, X-ray diffraction pattern and Raman spectra respectively. It showed GO paper has three types of electrical transitions as shown in Figure 2, in which the changes takes placed from -40°C to 150°C respectively. It is clearly showed that for below 10°C , the GO paper undergo insulating characteristics while at 10°C to 90°C it suddenly undergo conducting characteristics, afterwards at 90°C it then appear as insulating characteristics and increase to 100°C . From 100°C , another conducting transition appear in the result thus continue to conduct with increase of temperature.

The electrical conductivity of GO paper was determined based on the water molecule and impurity residue (hydrochloric acid was used for removing metallic ions during the GO purification process) at low temperatures [4]. When the temperature is lower than 10°C , the water molecules and impurities were 'freeze', thus GO paper experiencing insulating characteristic. From 10°C , the movement ability of water and impurity within the GO paper could be significantly increased thus resulting in increased electrical conductivity. The derivatives of graphene until it becomes single layer have been further discussed by N Saravanan et al [5].

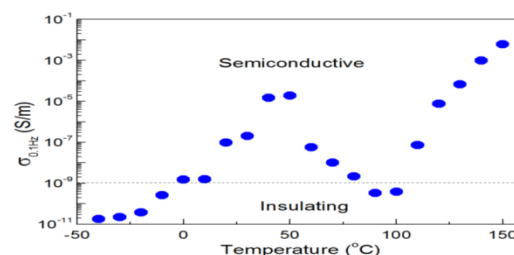


Figure 2. Electrical Transitions of GO Paper [4].

3. Polymethyl Methacrylate

PMMA is a transparent thermoplastic material. It is more widely used than other plastics due to its high light transmission, long service life, high ultraviolet light resistance and weathering, and good insulation properties. PMMA also has the greatest surface hardness of all thermoplastics. It can be fabricated by means of bulk polymerization, solution polymerization,

and radical polymerization since basically it is chemically a synthetic of methyl methacrylate. Another benefit of PMMA is that it is 100% recyclable, which provides a major contribution to saving natural resources. Several PMMA properties of note include breakdown potential properties of 16–30 kV/mm, dielectric loss factor of 0.04–0.06%, density of 1.18 g/cm³, melting point of 160°C, and boiling point of 200°C [6].

4. Fabrication and Application of PMM/GO

There are several methods to fabricate PMMA/GO nanocomposites. One technique fabricates a high nanofiller content of the GO solution and polymer host by using a simple membrane called the Vacuum Assisted Self Assembly (VASA); this technique can quickly produce macroscopic samples of a homogeneous layered GO-polymer nanocomposite with a hydrophilic or hydrophobic polymer. The VASA technique is easier, faster, less expensive, and has a wider material selection than the layer-by-layer assembly (LBL) technique [7].

Another method to fabricate a high-content nanofiller PMMA and GO is Pickering emulsion polymerization. The GO is synthesized using Hummers method from graphite powder. Subsequently, a certain amount of an oil phase, either xylene or MMA, is added to the AIBN mixture (200 ratio); this is followed by the addition of GO in an aqueous dispersion. The mixtures are emulsified using a sonicator for 5 min. The MMA emulsions are then polymerized at 70 °C for 6 h with stirring and then filtered to separate the nanocomposite powder, which is dried for 24 h. The emulsified GO is added to a commercial PMMA and subjected to melt mixing for 6 min. To ensure that neutralization of the charged groups in the structure of the GO does not cause coagulation of the GO/polymer particles, AIBN is used as an organic-soluble initiator for polymerization [8].

There are two techniques that use solvent processing to fabricate GO in polymeric materials [9]. The first is the direct dispersion of GO in water and using many organic solvents for the exfoliation of GO into GO layers. These GO sheets are then reduced to recover the sp² carbon network using solvents, such as sodium borohydride hydrazine, dimethylhydrazine, and ascorbic acid. Thermal expansion can also be used to enable exfoliation and reduction of GO into graphene layers by a simple and rapid heat treatment. Partially oxygenated graphene layers are produced when GO disperses readily in the polar solvents. This method is generally called the solvent-blending procedure. The second technique is in-situ polymerization. The chemically modified graphene is mixed with the monomers or pre-polymers, sometimes in the presence of a solvent, and the polymerization reaction takes place by adjusting temperature and time. The advantages of in-situ polymerization are it enables an outstanding and homogeneous dispersion and it provides a strong interaction between the incorporated particles and the polymer matrix, facilitating stress transfer. However, this process usually results in enhanced viscosity, which hinders manipulation and loading fraction.

In the melt-blending method, the GO is included in the melted polymer using a twin-screw extruder and adjusting parameters, such as screw speed, temperature, and time. The fabrication of GO/PMMA also has been reported using dispersion polymerization [10]. Basically, GO is synthesized using Hummers method, and a monodispersed PMMA is synthesized using dispersion polymerization.

5. PMMA/GO Simulation Model

In order to validate that the PMMA/GO has a better dielectric strength than pure PMMA, we carried out a simulation study. The purpose of the study was to observe the electric potential distribution dissimilarity between PMMA/GO and a pure PMMA sample when a void is exhibited. In Figure 3, the construction of a 2D model of PMMA/GO with a void is described. The large circle represents the high steel conductor. For the rectangular geometry shown in Figure 3, different materials have been defined: (1) PMMA polymer, (2) GO nanofiller, and (3) the voids. The thickness and width of the PMMA is 1 mm × 30 mm, the void is 0.1 mm × 38 mm, and the GO is 0.001 mm × 2 mm.

If the field exists in a region consisting of different media, the conditions that the field must satisfy at the interface separating the media are called boundary conditions. The conditions are dictated by the types of material the media are made of.

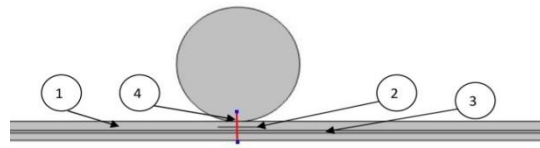


Figure 3. Two-Dimensional Model of PMMA/GO (see text for explanation; no. 4 indicates the cutline)

The boundary condition at a separating interface should consider the following: dielectric (ϵ_{r1} dan dielectric (ϵ_{r1}); conductor and dielectric; conductor and free space. To determine the boundary conditions, Maxwell's equation for electrostatic properties is used as follows:

$$\oint \mathbf{E} \cdot d\mathbf{l} = 0 \quad (1)$$

and

$$\oint \mathbf{D} \cdot d\mathbf{S} = Q_{enc} \quad (2)$$

The electric field intensity \mathbf{E} is decomposed into two orthogonal components,

$$\mathbf{E} = \mathbf{E}_t + \mathbf{E}_n \quad (3)$$

where \mathbf{E}_t and \mathbf{E}_n are the tangential and normal components of \mathbf{E} to the interface of interest, respectively. A similar decomposition can be done for the electric flux density \mathbf{D} .

The relation between applied voltage (V) and electric field (\mathbf{E}) is shown in Equation 4 as:

$$\mathbf{E} = -\nabla V \quad (4)$$

Then, the relationship of \mathbf{E} with the current displacement (\mathbf{D}) is affected by the permittivity of the insulation material ($\epsilon = \epsilon_0 \epsilon_r$), as shown in Equation 5 as:

$$\mathbf{D} = \epsilon \mathbf{E} \quad (5)$$

Gauss' law states that charge density (ρ) is equal to gradient \mathbf{D} , as shown in Equation 6.

$$\nabla \cdot \mathbf{D} = \rho \quad (6)$$

However, from the electric charge density (ρ), a flux (\mathbf{J}) can be obtained by using Equation 7, in which Q is the electric charge as follows:

$$\nabla \cdot \mathbf{J} = \mathbf{Q} \cdot \mathbf{j} = -\partial \rho / \partial t \quad (7)$$

$$\mathbf{J} = \sigma \mathbf{E} + \partial \mathbf{D} / \partial t + \mathbf{J}_e \quad (8)$$

Equation 9 can be obtained from Equation 6 and Equation 7 as follows:

$$\nabla \cdot (\mathbf{J} + \partial \mathbf{D} / \partial t) = 0 \quad (9)$$

By substituting Equation 5 and Equation 8 in Equation 9, then replacing \mathbf{E} with Equation 4, we obtain Equation (10)

$$-\nabla \cdot (\sigma + (\partial \epsilon / \partial t)) \nabla V = 0 \quad (10)$$

Equation 4 to Equation 10 are used to calculate the potential distribution of the constructed model by using the finite element method (FEM) [11-12]. All calculation proses from mesh generating to electric potential distribution mapping were carried out by using COMSOL Multiphysic. Mesh generating of the PMMA/GO model is shown in Figure 4.

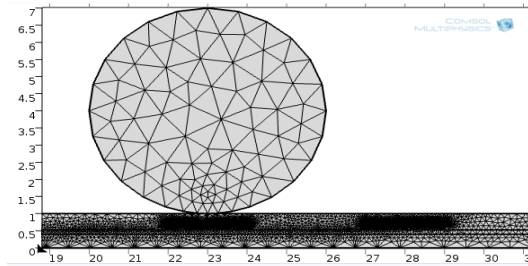


Figure 4. Mesh Result for PMMA/GO Sample

6. Results and Discussion

It is necessary to identify the electric potential and electric field when a void is introduced in order to identify which samples will give the worst case. Figure 3 shows the length of the simulation model at the y-axis; represents the location of the void thickness. The void thickness is 0.4-0.5 mm at the y-axis. Figures 5-7 show the line graph of the electric potential versus the y-coordinate of the simulation model. From these three figureures, the electric potential is shown to be decreasing from its initial value of the injected voltage to zero. Figure 5 shows the electric potential when the void is not introduced; this shows that the value steadily decreases from 5 kV to 0 V. However, Figure 6 shows that the electric potential decreases in the GO. Hence the electric potential at the PMMA/GO nanocomposite is much less when it crosses the sample as compared to pure PMMA with and without the void. In Figure 6, the electric potential at 0.9 mm length is 3.05 kV while the rest are 4.2 kV (Figure 5) and 3.4 kV (Figure 7).

On the other hand, Figure 8 and Figure 9 show the results of the electric field versus the y-coordinate for PMMA/GO and the pure PMMA sample. From these figureures, the electric field in the conductor area gives a high value compared to the lower part of those samples, indicating that the electric field is proportional to electric potential. The electric field value increases as the injected voltage increases. As shown in Figure. 8, for a 5-kV input at 0.4 mm length, the electric field is 0.62×10^7 V/m. The difference between the PMMA/GO nanocomposite and pure PMMA is evident at the void where the line for pure PMMA is thicker compared to that of the PMMA/GO composite.

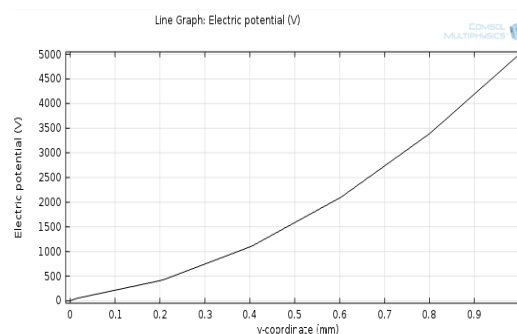


Figure 5. Electric Potential for Pure PMMA when no Void is Introduced

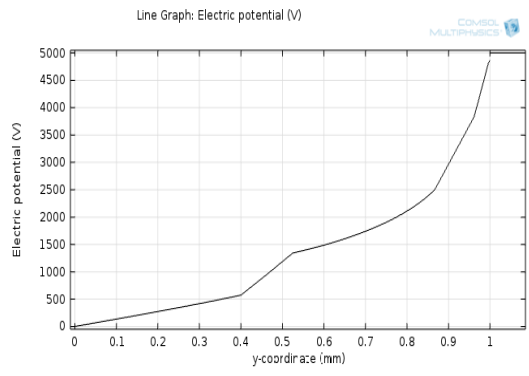


Figure 6. PMMA/GO Electric Potential.

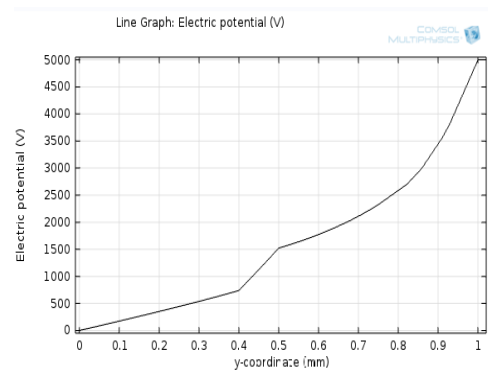


Figure 7. Electric potential for Pure PMMA when a Void is Introduced.

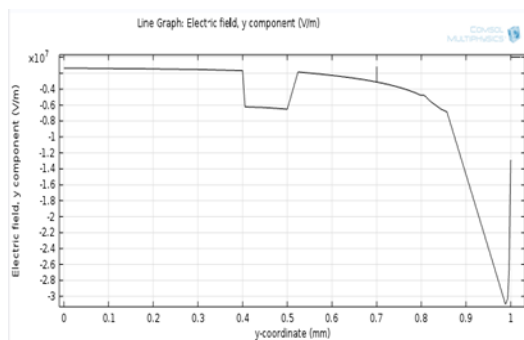


Figure 8. PMMA/GO Line Graph for an Fi Electric Field at 5-kV Input

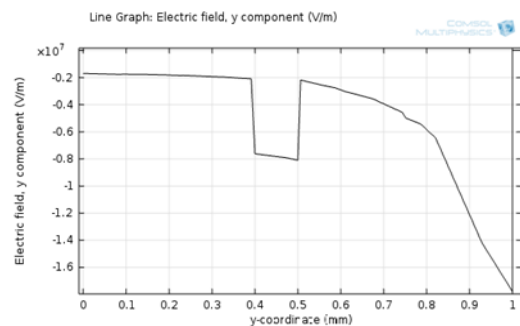


Figure 9. Pure PMMA Line Graph for an Electric Field at 5-kV Input.

PD occurs at the void but happens so quickly (in nanoseconds) that its simulation may not be captured; however, the characteristics of the electric field are taken into account. The ionization processes are initiated in the void, and due to the electric field, the ions and electrons start to move and begin charge separation. Moreover, due to their small weight, electrons can accelerate to almost the speed of light. As in the electrodes, the charge separation appears as a small amount of charge and accordingly a small current impulse. At the location of the PD, the current impulse has a very short duration, in orders of nanoseconds [13].

7. Conclusion

PMMA/GO nanocomposite fabrication and application have been described, and we carried out a simulation of the electric potential and electric field characteristics of pure PMMA and a PMMA/GO nanocomposite with and without voids by using FEM. The results show that when there is a void, the PMMA/GO nanocomposite characteristics in terms of electrical potential and electric field are improved compared with those of pure PMMA. In the future, a laboratory experiment to observe the characteristics of the PMMA/GO nanocomposite in relation to PD development on solid material will be carried out.

Acknowledgment

The authors would like to thank *Universiti Teknologi Malaysia* and *Universitas Sriwijaya* for the facilities and financial support. Under Research University Grant and Research Collaboration Grant.

References

- [1] S Stankovich, DA Dikin, GH Dommett, KM Kohlhaas, EJ Zimney, EA Stach, *et al.* Graphene-Based Composite Materials. *Nature*. 2016; 442; 282-286.
- [2] H Kim, AA Abdala, CW Macosko. Graphene/Polymer Nanocomposites. *Macromolecules*. 2010; 43: 6515-6530.
- [3] DA Dikin, S Stankovich, EJ Zimney, RD Piner, GH Dommett, G Evmenenko, *et al.* Preparation and Characterization of Graphene Oxide Paper. *Nature*. 2007; 448: 457-460.
- [4] X Huang, F Liu, P Jiang, T Tanaka. *Is Graphene Oxide an Insulating Material?*. IEEE International Conference on Solid Dielectrics (ICSD). 2013; 904-907.
- [5] N Saravanan, R Rajasekar, S Mahalakshmi, T Sathishkumar, K Sasikumar, S Sahoo. Graphene and modified graphene-based polymer nanocomposites: A review. *Journal of Reinforced Plastics and Composites*. 2014; 33: 1158-1170.
- [6] MATBASE. (19 April). *Polymethyl Methacrylate (PMMA)*. Available: <http://www.matbase.com/material-categories/natural-and-synthetic-polymers/commodity-polymers/material-properties-of-polymethyl-methacrylate-extruded-acrylic-pmma.html>
- [7] KW Putz, OC Compton, MJ Palmeri, ST Nguyen, LC Brinson. High-Nanofiller-Content Graphene Oxide-Polymer Nanocomposites via Vacuum-Assisted Self-Assembly. *Advanced Functional Materials*. 2010; 20: 3322-3329.
- [8] MM Gudarzi, F Sharif. Self assembly of graphene oxide at the liquid–liquid interface: a new route to the fabrication of graphene based composites. *Soft Matter*. 2011; 7: 3432-3440.
- [9] R Verdejo, MM Bernal, LJ Romasanta, MA Lopez-Manchado. Graphene filled polymer nanocomposites. *Journal of Materials Chemistry*. 2011; 21: 3301-3310.
- [10] K Zhang, WL Zhang, HJ Choi. Facile fabrication of self-assembled PMMA/graphene oxide composite particles and their electroresponsive properties. *Colloid and Polymer Science*. 2013; 291: 955-962.
- [11] D Smith, SG McMeekin, BG Stewart, P Wallace. *Transformer bushings Modelling of electric field and potential distributions within oil impregnated paper with single and multiple spherical cavities*. in Universities Power Engineering Conference (UPEC). 45th International. 2010; 1-6.
- [12] S Tupsie, A Isaramongkolrak. Analysis of electromagnetic field effects using FEM for transmission lines transposition. 2009.
- [13] M Naidu, V Kamaraju. High Voltage Engineering. 3rd ed: Mc Graw Hill. 2004.